Insertion of SO_2 into the Metal−Carbon Bonds of Rhodium and Iridium Compounds, and Reactivity of the SO_2-Inserted Species

Laurent Lefort, Rene J. Lachicotte, and William D. Jones*

Department of Chemistry, University of Rochester, Rochester, New York 14627

Received November 21, 1997

Sulfur dioxide has been found to insert into the metal−carbon bonds of both rhodium and iridium alkyl and aryl complexes. The sulfinate ligand can be removed with a strong acid such as HCl, generating free sulfinic acid. Acids with weakly coordinating anions protonate the sulfinate oxygen, but the sulfinic acid remains bound to the metal center. Added sulfinic acids can exchange with the coordinated sulfinate group.

Introduction

The insertion of SO_2 into M−C bonds has been studied extensively during the 1960's and 1970's.[1] Many transition-metal alkyl and aryl complexes have been shown to undergo this reaction, and several types of linkages have been observed. A mechanism has been proposed that still holds in the majority of cases.[1a] While current interest in this reaction has decreased, SO_2 remains the subject of numerous studies[2] because of its diverse coordination properties and its role in acid rain production.

In this paper, we present two new systems that are able to cleanly insert SO_2 into their M−C bonds. Both are based on group VIII metal complexes containing an aryl or alkyl ligand. The reactivities of the SO_2-inserted species have been studied, and we have shown that it is possible to release the RSO_2 group from the metal to form sulfinic acids.

Results and Discussion

SO_2 Insertion into Rhodium Complexes. Addition of 1 atm of SO_2 to a solution of Cp*Rh(PMe_3)(Cl)(C_6H_5) (**1a**) in CH_2Cl_2 leads to the quantitative formation (based on the NMR) of a new product (**2a**) after 4 h at room temperature. The orange solution does not change color during the course of the reaction, and no intermediates can be seen while monitoring the reaction by ^{1}H NMR spectroscopy. The ^{1}H NMR spectrum of the product **2a** exhibits both Cp* and PMe_3 resonances, but in contrast to the spectrum of the starting material, the PMe_3 resonance (δ 1.70) appears downfield relative to the Cp* peak (δ 1.50). In the aromatic region of the spectrum, two multiplets are observed at δ 7.39 and 7.89. The ^{31}P NMR spectrum of **2a** has a doublet with $J_{Rh-P} = 140$ Hz, consistent with a Rh(III) compound.[3]

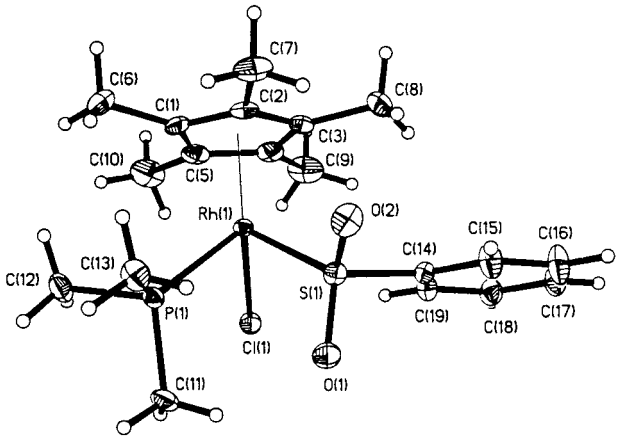

Figure 1. ORTEP drawing of Cp*Rh(PMe_3)(SO_2Ph)(Cl), **2a**. Ellipsoids are shown at the 30% level.

Crystals of **2a** have been obtained by layering a solution of **2a** in methylene chloride with hexane. The X-ray structure (Figure 1) shows that SO_2 insertion has occurred into the C−M bond in a [1,1] fashion, giving a S-sulfinate (eq 1). Crystallographic data are listed in

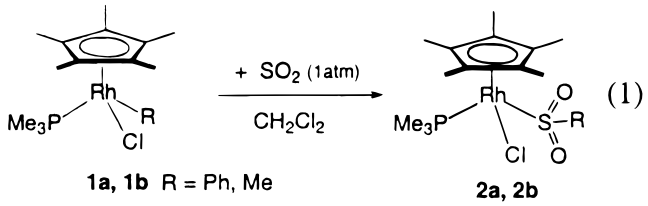

(1)

Table 1, and selected distances and angles are given in Table 2.

A solution of Cp*Rh(PMe_3)(Cl)(CH_3) (**1b**) in CH_2Cl_2 was found to undergo a similar reaction in the presence of 1 atm of SO_2. Despite the absence of a color change, ^{1}H NMR spectroscopy shows the complete disappearance of the starting material after 10 min at room temperature and the clean formation of a new product (**2b**). The ^{1}H NMR spectrum of **2b** shows both Cp* and PMe_3 resonances. The CH_3 resonance in **2b** appears as

(1) (a) Wojcicki, A. *Adv. Organomet. Chem.* **1974**, *12*, 31. (b) Alexander, J. J. In *The Chemistry of Metal Carbon Bond*; Patai, S., Ed.; Wiley: New York, 1985; Vol. 2. (c) Wong, C. W.; Kitching, W. *J. Organomet. Chem.* **1970**, *22*, 102. (d) Gupta, B. D.; Roy, M.; Oberoi, M.; Dixit, V. *J. Organomet. Chem.* **1992**, *430*, 197−204. (e) Joseph, M. F.; Baird M. C. *Inorg. Chim. Acta* **1985**, *96*, 229−230.

(2) Kubas, J. K. *Acc. Chem. Res.* **1994**, *27*, 183−190.

(3) Klingert, B.; Werner, H. *Chem. Ber.* **1983**, *116*, 1450−1462.

S0276-7333(97)01030-3 CCC: $15.00
Publication on Web 03/05/1998

Table 1. Summary of Crystallographic Data for 2a, 2b, and 6

	2a	2b	6
	Crystal Parameters		
chem formula	$C_{19}H_{29}ClO_2PRhS$	$C_{14}H_{27}ClO_2PRhS$	$C_{17}H_{30}F_3IrNO_5PS_2$
fw	490.81	428.75	672.71
cryst syst	orthorhombic	orthorhombic	tetragonal
space group	$P2_12_12_1$ (No. 19)	$Pna2_1$ (No. 33)	$I4_1/a$ (No. 88)
Z	4	4	16
a, Å	9.9742(6)	24.511(4)	16.9846(4)
b, Å	14.3780(9)	8.5740(13)	16.9846(4)
c, Å	15.1600(9)	8.5845(13)	33.4343(11)
vol., Å^3	2174.1(2)	1804.1(5)	9645.0(5)
ρ_{calc}, g cm^{-3}	1.50	1.58	1.853
cryst dimens, mm	0.29 × 0.35 × 0.35	0.36 × 0.38 × 0.40	0.20 × 0.30 × 0.40
temp, °C	−80	−80	−80
	Measurement of Intensity Data		
diffractometer	Siemens SMART	Siemens SMART	Siemens SMART
radiation	Mo Kα, 0.710 73	Mo Kα, 0.710 73	Mo Kα, 0.710 73
2θ range, deg	4.0−56.4	3.4−56.4	2.7−56.6
data collected	$-12 \le h \le 13$, $-12 \le k \le 18$, $-20 \le l \le 18$	$-32 \le h \le 32$, $-11 \le k \le 11$, $-6 \le l \le 11$	$-21 \le h \le 22$, $-16 \le k \le 22$, $-44 \le l \le 41$
no. of data collected	11 506	10 802	28 131
no. of unique data	4960	3246	5816
agreement between equiv data	0.024	0.037	0.047
no. of obsd data	4721 ($I > 2\sigma(I)$)	2969 ($I > 2\sigma(I)$)	5137 ($I > 2\sigma(I)$)
no. of params varied	227	181	272
μ, cm^{-1}	1.088	1.298	5.827
abs corr	empirical (SADABS)	empirical (SADABS)	empirical (SADABS)
range of trans. factors	0.87−1.00	0.76−0.93	0.63−0.93
R1(F_o), wR2(F_o2), ($I > 2\sigma(I)$)	0.0250, 0.0597	0.0396, 0.0663	0.0816, 0.1869
R1(F_o), wR2(F_o2) (all data)	0.0274, 0.0606	0.0455, 0.0678	0.0955, 0.1920
goodness of fit	1.15	1.21	1.48

Table 2. Selected Distances (Å) and Angles (deg) for 2a, 2b, and 6

	2a, M = Rh	**2b**, M = Rh	**6**, M = Ir
	Distances		
M−S(1)	2.3161(6)	2.3266(13)	2.334(3)
S(1)−O(1)	1.467(2)	1.463(4)	1.477(9)
S(1)−O(2)	1.468(2)	1.442(5)	1.466(9)
S(1)−C(14)	1.808(3)	1.805(7)	1.782(13)
M−P(1)	2.3077(6)	2.2989(14)	2.317(3)
M-Cl(1) or M−N(1)	2.4019(6)	2.405(2)	2.031(9)
	Angles		
M−S(1)−O(1)	115.64(9)	115.8(2)	113.6(4)
M−S(1)−O(2)	109.49(9)	111.0(2)	111.3(4)
M−S(1)−C(14)	102.91(12)	106.8(2)	109.9(5)
O(1)−S(1)−O(2)	112.97(14)	113.2(3)	113.1(6)
O(1)−S(1)−C(14)	102.91(12)	104.3(3)	105.3(7)
O(2)−S(1)−C(14)	103.63(13)	104.6(3)	102.9(6)
P(1)-M−S(1)	88.14(2)	88.53(5)	89.64(11)

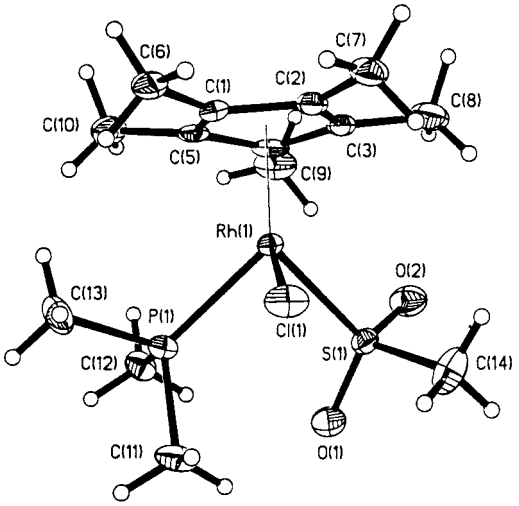

Figure 2. ORTEP drawing of Cp*Rh(PMe_3)(SO_2CH_3)(Cl), **2b**. Ellipsoids are shown at the 30% level.

a singlet instead of a doublet of doublets, and its chemical shift (δ 2.83) is close to that observed for methane sulfinic acid (δ 2.68), CH_3SO_2H. The coupling constant of the doublet observed in the ^{31}P spectrum of **2b** (J_{Rh-P} = 144 Hz) shows that no change in the oxidation state of the metal has taken place during the reaction.

Again, crystals have been grown from slow diffusion of hexane into a methylene chloride solution of **2b**. The crystal structure (Figure 2) confirms the formation of a S-sulfinate. Crystallographic data are given in Table 1, and selected distances and angles are given in Table 2.

In both of these 18-electron, coordinatively saturated complexes, the insertion of SO_2 into the carbon−metal bond occurs selectively to give S-bound sulfinates. The mechanism of insertion likely involves the electrophilic attack of SO_2 on the M−C bond, as postulated for several similar compounds.[1a] Consistent with this mechanism is the fact that the reaction is much faster with the methyl complex than with the phenyl complex (the latter being more sterically hindered for a backside attack and less electron-donating).

SO_2 Insertion into Iridium Complexes. As an analogue of complex **1b**, the iridium complex Cp*Ir(PMe_3)(Cl)(CH_3) (**3**) has been synthesized and reacted with 1 atm of SO_2 in CH_2Cl_2 at room temperature. The reaction is not clean and gives several unidentified compounds. This behavior is different from that observed with Rh and might result from the instability of **3**, which tends to disproportionate into a mixture of the iridium dimethyl and dichloride complexes upon standing in solution. SO_2 insertion could then also occur into the dimethyl complex, leading either to the mono or the bis S-sulfinate, and thereby accounting for the mixture of products obtained.

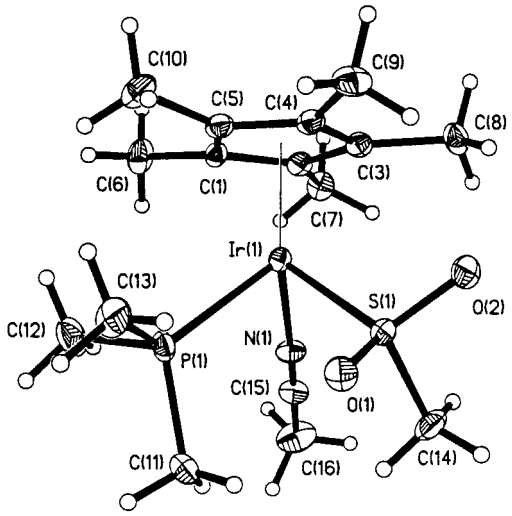

Figure 3. ORTEP drawing of $[Cp^*Rh(PMe_3)(SO_2CH_3)(CH_3CN)]^+[OTf]^-$, **6**. Ellipsoids are shown at the 30% level. The triflate ligand has been omitted for clarity.

$Cp^*Ir(PMe_3)(OTf)(CH_3)$ (**4**) is very similar to **3** but is more stable toward disproportionation. Indeed, one way to synthesize this compound is to react 1 equiv of $Cp^*Ir(PMe_3)(CH_3)_2$ with 1 equiv of $Cp^*Ir(PMe_3)(OTf)_2$.[4] When a solution of **4** in CH_2Cl_2 is put under an atmosphere of SO_2 at room temperature, the orange solution immediately turns yellow. The ^1H NMR spectrum shows the quantitative formation of a new product (**5**), with both Cp* and PMe_3 resonances. As in the case of the phenylrhodium compound **2a**, the PMe_3 resonance of **5** (δ 1.79) appears downfield relative to the Cp* peak (δ 1.75) and the CH_3 peak appears as a singlet at δ 2.77 ppm, close to a methyl resonance in methane sulfinic acid. These spectroscopic observations provide good evidence for **5** being the SO_2-inserted compound. Due to its lack of stability, however, crystals of **5** have not been obtained.

Acetonitrile has been observed to be capable of displacing the labile triflate ligand in other organometallic systems.[5] Reaction of **5** with an excess of CH_3CN in CH_2Cl_2 leads to an immediate color change of the solution from yellow to colorless. Removal of the excess of acetonitrile under vacuum leaves a white solid (**6**). The ^1H NMR spectrum of **6** is consistent with an acetonitrile adduct, exhibiting two methyl resonances (3 H each) in the region 2.5−3 ppm (δ 2.98, s; 2.82, d, J = 1.6 Hz). **6** is much more stable than **5**, and crystals have been grown from toluene solution at −40 °C. The crystal structure of **6** (Figure 3) shows that SO_2 has inserted in a [1,1] fashion into the M−C bond of **4**. Crystallographic data are listed in the Table 1, and selected distances are listed in Table 2. Equation 2 summarizes the reaction sequence. It is interesting to

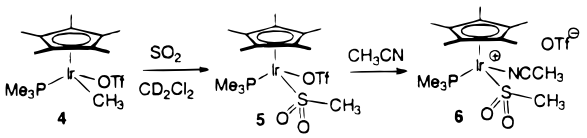

(2)

note that despite its lability, the triflate ligand is not displaced by SO_2.

(4) Burger, P.; Bergman, R. G. *J. Am. Chem. Soc.* **1993**, *115*, 10462.

Reaction of SO_2 Insertion Complexes of Rhodium with Acids. As the SO_2 insertion reaction represents a way to functionalize an alkyl or aryl group bound to a metal, the release of the sulfinate group was also investigated previously. In the case of Mn compounds, this has been accomplished by oxidative demetalation.[6] The SO_2-inserted species was reacted with H_2O_2, leading to the formation of MnO_2 and a mixture of sulfinate and sulfonate products. The breaking of the metal−sulfur bond can also be induced by reacting the SO_2-inserted compound with an acid, as seen in the case of alkyl−copper reagents, to give the corresponding sulfinic acids.[7]

When **2a** or **2b** is reacted with aqueous HCl in THF solution, the ^1H NMR spectrum shows the quantitative formation of $Cp^*Rh(PMe_3)(Cl)_2$ and free sulfinic acid, RSO_2H (R = C_6H_5 for **2a**, R = CH_3 for **2b**) (eq 3).

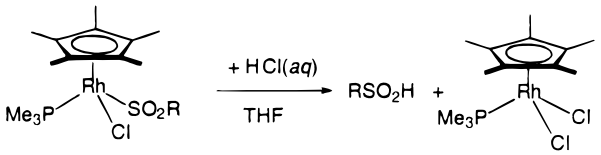

(3)

2a, 2b R = Ph, Me

$Cp^*Rh(PMe_3)(Cl)_2$ was identified by its ^1H and ^{31}P spectra. Authentic samples of the sulfinic acids were synthesized from their commercially available Na salts, and their ^1H NMR spectra matched with those obtained in the reaction of **2a** or **2b** with aqueous HCl. The reactions between the Rh compounds and HCl are not a simple ligand substitution by chloride ion. No reaction has been observed between **2a** or **2b** and a chloride source such as NaCl.

Nevertheless, the anion of the acid plays a crucial role in the formation of free sulfinic acid. Indeed, the use of acids with noncoordinating anions such as HOTf (HOTF = CF_3SO_3H, triflic acid) or HBF_4 does not lead to the production of free sulfinic acids. The orange solution of (**2b**) in methylene chloride gradually turns red as an increasing amount of triflic acid is added. The ^1H NMR spectrum shows the chemical shift of the methyl group progressively moving downfield according to the amount of added triflic acid, up to 1 equiv of added acid. Addition of more than 1 equiv of acid results in no further change in the chemical shift. Small changes are also observed in the chemical shifts of the Cp* and PMe_3 resonances upon addition of triflic acid, but the most obvious change is a broadening of the resonances. This effect becomes even more obvious in the ^{31}P NMR spectrum, where the well-resolved doublet is replaced by a broad hump upon addition of 1.5 equiv of triflic acid.

The compound formed by reacting **2b** with 1 equiv of triflic acid, **7a**, is not the chloro−triflate complex, $Cp^*Rh(PMe_3)(Cl)(OTf)$ (**8**). This latter compound can be synthesized independently by reaction of the methyl chloride complex $Cp^*Rh(PMe_3)(Cl)(CH_3)$ with 1 equiv of triflic acid and displays different NMR resonances to those of **7a**.

(5) Stang, P. J.; Huang, Y.-H.; Arif, A. M. *Organometallics* **1992**, *11*, 231−237.

(6) Cooney, J. M.; Depree, C. V.; Main, L.; Nicholson, B. K. *J. Organomet. Chem.* **1996**, *515*, 109−118.

(7) Cahiez, G.; Bernard, D.; Normant, J. F.; Villiers, J. *J. Organomet. Chem.* **1976**, *121*, 123−126.

Upon addition of 2 equiv of HBF_4 to a solution of **2b** in CH_2Cl_2, a compound, **7b**, with NMR properties similar to those of **7a** can be produced. The chemical shift of the methyl group in **7b** (δ 3.23) is the same as that for **7a**, and its ^{31}P NMR spectrum also appears as a broad hump. This last experiment suggests that the anion (OTf^- for **7a**, BF_4^- for **7b**) might not be bound to the metal. Were this not the case, a greater difference would be expected in the ^1H spectra of **7a** and **7b**.

Reaction of **7a** or **7b** with an excess of dry Et_3N regenerates **2b**. Consequently, it appears the compounds **7a** and **7b** are protonated derivatives of **2b**, the protonation being reversible in the presence of a base. No hydride resonances were observed in the ^1H NMR spectra of **7a** and **7b**, showing that the protonation does not occur directly on the metal. The most likely position for protonation in the complexes are the oxygens of the sulfinate group, giving an acidic proton, which is consistent with an observed broad peak at chemical shifts between 10 and 13 ppm. The possibility of an interaction between the oxygen of a RSO_2 group bound to a metal and a Lewis acid has been previously observed by Wojcicki.[8] The W complex $CpW(CO)_3(S(O)_2CH_3)$ forms a 1:1 adduct with BF_3, formulated as $CpW(CO)_3(S(O)(OBF_3)CH_3)$. These arguments lead to the proposed formulation for **7a** or **7b** as $Cp^*Rh(PMe_3)(Cl)(S(O)(OH)CH_3)^+X^-$ ($X^- = OTf^-$ for **7a**, BF_4^- for **7b**). In these complexes, the change in the chemical shift of the methyl group with added acid can be explained by a rapid exchange of the proton between the protonated and the nonprotonated species (eq 4).

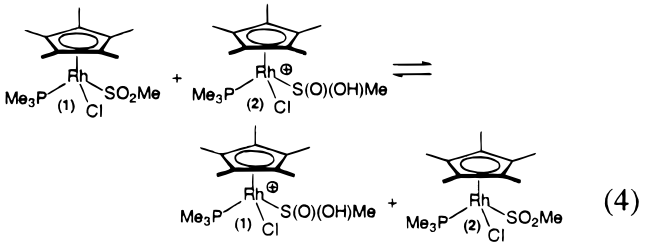

(4)

In the rapid exchange limit, the peak for the methyl group will appear at a position intermediate between that in the protonated species and the nonprotonated species. When more than 1 equiv of acid has been added, all the species will be protonated but rapid exchange with the excess acid can occur.

Independent synthesis of **7a** confirms this formulation. Addition of 1 equiv of methane sulfinic acid to a solution of chloro triflate compound **8** in CH_2Cl_2 leads to an immediate color change from red to orange. The ^1H and ^{31}P NMR spectra indicate that **7a** is quantitatively formed. If the sodium salt of methane sulfinic acid is used instead of the acid, compound **2b** is quantitatively formed overnight, showing again that **2b** and **7a** differ by only a proton. A summary of these reactions are shown in Scheme 1.

The above results show that the reaction of **2b** with an acid can follow two different pathways depending on the coordination properties of the acid counterion. In the first case (HCl), the rhodium compound formed

Scheme 1

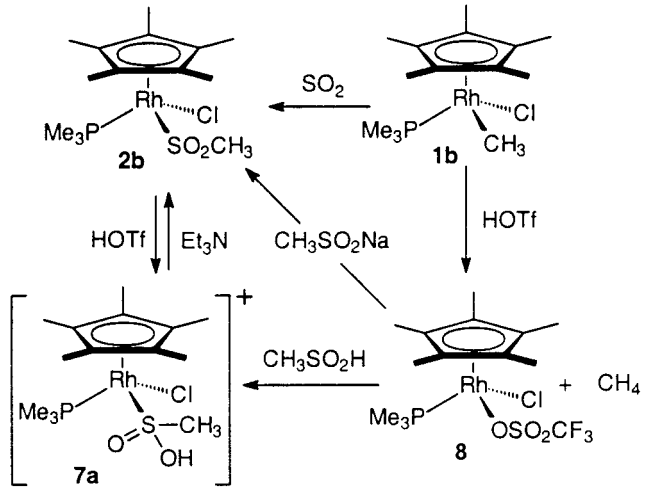

($Cp^*Rh(PMe_3)(Cl)_2$) was a stable species, unable to bind the free methane sulfinic acid. In the second case (HOTf, HBF_4), the inability to form a strong bond between the metal and the labile counterion prevented the release of free sulfinic acid. A third case can be imagined corresponding to an intermediate situation, where the Rh compound formed after reaction with the acid can back-react with the free sulfinic acid, leading to an equilibrium between free and bound acids. To observe such behavior, it would be necessary to use a counterion that can bind to the metal with a bond energy close to that of the methyl sulfinic acid. A different sulfinic acid nicely fulfills this requirement.

The addition of 1.1 equiv of phenyl sulfinic acid to a solution of **2b** in CH_2Cl_2 gives, after 2 h of reaction, a mixture with a constant composition containing **2a**, **2b**, methane sulfinic acid, and phenyl sulfinic acid. All products can be identified by their ^1H NMR spectra. Integration allows calculation of an equilibrium constant, K_{eq}, of 0.59. The addition of more phenyl sulfinic acid leads to the consumption of more **2b**, and a similar value for the equilibrium constant is obtained (K_{eq} = 0.57) once the composition of the mixture stops changing. This behavior confirms the existence of the equilibrium in eq 5.

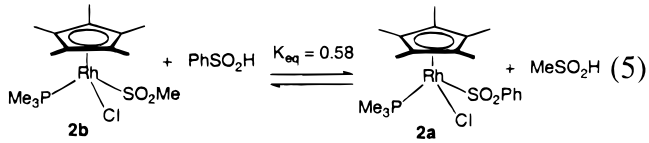

(5)

The equilibrium constant obtained can be compared to that for the equilibrium between the sulfinic acids and their conjugate bases (eq 6). Note that the K_{eq} for

$$MeSO_2^- + PhSO_2H \underset{}{\overset{K_{eq} = 9.8}{\rightleftharpoons}} PhSO_2^- + MeSO_2H \qquad (6)$$

the rhodium-bound sulfinate is about 20 times smaller than the equilibrium constant obtained for the pure acids. This difference can be attributed to the difference in rhodium−sulfur bond strengths in **2a** vs **2b** and consequently shows that the methyl sulfinate bond is stronger than the phenyl sulfinate bond.

(8) Severson, R. G.; Wojcicki, A. *J. Am. Chem. Soc.* **1979**, *101*, 877−883.

Conclusion

Two new transition-metal compounds have been found to undergo a clean SO_2 insertion in their M−C bonds. For both of these compounds, the reaction occurs under mild conditions (room temperature, 1 atm of SO_2) and appears to be quantitative. The reactions of the Rh-inserted species with different kinds of acids allows us to propose the following mechanism for the formation of free sulfinic acids. The first step involves the protonation of one of the oxygens of the SO_2 group. The coordinated RS(O)(OH) group (a sulfinic acid) is much more labile than the sulfinate group and can be displaced in a second step by the acid counterion, provided the latter exhibits some coordination properties toward the metal. Depending upon the acid reagent, it has been possible to obtain a sulfinic acid either free in solution or bound to the rhodium as a ligand.

Experimental Section

General Considerations. All manipulations were performed under an N_2 atmosphere, either on a high-vacuum line using modified Schlenk techniques or in a Vacuum Atmospheres Corp. glovebox. Tetrahydrofuran, benzene, and toluene were distilled from dark purple solutions of benzophenone ketyl. Acetonitrile was distilled from a solution of CaH_2. Alkane solvents were made olefin-free by stirring over H_2SO_4, washing with aqueous $KMnO_4$ and water, and distilling from dark purple solutions of tetraglyme/benzophenone ketyl. Dichloromethane-d_2 was purchased from Cambridge Isotope Lab., dried over CaH_2, distilled under vacuum, and stored in ampules with Teflon-sealed vacuum line adaptors. The preparations of $Cp^*Rh(PMe_3)(CH_3)(Cl)$,[9] $Cp^*Rh(PMe_3)(Ph)(Cl)$,[9] $Cp^*Ir(PMe_3)(CH_3)(Cl)$,[10] and $Cp^*Ir(PMe_3)(CH_3)(OTf)$[4] have been previously reported. CH_3SO_2Na, $PhSO_2Na$, CF_3SO_3H, and HBF_4 were purchased from Aldrich Chemical Co. SO_2 was purchased from Air Products and Chemicals Inc. and used without further purification.

All ^1H NMR and ^{31}P NMR spectra were recorded on a Bruker AMX400 spectrometer. All ^1H chemical shifts are reported in ppm (δ) relative to tetramethylsilane and referenced using the chemical shifts of residual solvent resonances (C_6H_6, δ 7.15). ^{31}P NMR spectra were referenced to external 30% H_3PO_4 (δ 0.0). Analyses were obtained from Desert Analytics. A Siemens SMART CCD area detector diffractometer equipped with an LT-2 low-temperature unit was used for X-ray crystal structure determination.

Reaction of $Cp^*Rh(PMe_3)(Ph)(Cl)$ (1a) with SO_2. A 13 mg (0.03 mmol) amount of $Cp^*Rh(PMe_3)(Ph)(Cl)$ (**1a**) was dissolved in about 1 mL of dry, oxygen-free CH_2Cl_2-d_2. The solution was put into an NMR tube equipped with a Teflon seal and connected to a high-vacuum line. The solution was frozen and freeze−pump−thaw-degassed 3 times. The high-vacuum line was filled with 1 atm of SO_2, and the NMR tube was briefly opened to the SO_2 atmosphere. After 4 h at room temperature, **1a** had been quantitatively converted to $Cp^*Rh(PMe_3)(S(O)_2Ph)(Cl)$ (**2a**), as determined by NMR spectroscopy. The product was isolated by removal of the solvent under vacuum and recrystallized from CH_2Cl_2/hexane. ^1H NMR (400 MHz, CD_2Cl_2): δ 1.50 (d, J_{P-H} = 3.2 Hz, Cp*), 1.70 (dd, $J_{P,Rh-H}$ = 11.6, 0.8 Hz, PMe_3), aromatic resonances 7.35−7.42 (m, 3H), 7.86−7.91 (m, 2H). ^{31}P NMR (400 MHz, CD_2Cl_2): δ 10.44 (d, J_{Rh-P} = 140 Hz). Anal. Calcd for $C_{19}H_{29}ClO_2PRhS$: C, 46.48; H, 5.91. Found: C, 46.49; H, 5.88.

Reaction of $Cp^*Rh(PMe_3)(CH_3)(Cl)$ (1b) with SO_2. Complex **2b** was obtained similar to **2a** by reaction of $Cp^*Rh(PMe_3)(CH_3)(Cl)$ (**1b**) with 1 atm of SO_2 in CD_2Cl_2. The reaction goes to completion in 10 min at room temperature and is quantitative by NMR spectroscopy. ^1H NMR (400 MHz, CD_2Cl_2): δ 1.63 (d, J_{P-H} = 11.6 Hz, PMe_3), 1.70 (d, J_{P-H} = 3.2 Hz, Cp*), 2.83 (s, CH_3). ^{31}P NMR (400 MHz, CD_2Cl_2): δ 11.24 (d, J_{Rh-P} = 144 Hz). Anal. Calcd for $C_{14}H_{27}ClO_2PRhS$: C, 39.21; H, 6.30. Found: C, 39.00; H, 6.31.

Reaction of $Cp^*Ir(PMe_3)(CH_3)(OTf)$ (4) with SO_2. The procedure is the same as for **1a**, except that the pressure of SO_2 was reduced to 10−20 cmHg. A quantitative yield (according to NMR) of $Cp^*Ir(PMe_3)(SO_2CH_3)(OTf)$ (**5**) was obtained after a few minutes of reaction. ^1H NMR (400 MHz, CD_2Cl_2): δ 1.75 (d, J_{P-H} = 2.0 Hz, Cp*), 1.79 (d, J_{P-H} = 11.6 Hz, PMe_3), 2.77 (s, CH_3). ^{31}P NMR (400 MHz, CD_2Cl_2): δ −17.32 (s).

Reaction of $Cp^*Ir(PMe_3)(SO_2CH_3)(OTf)$ (5) with CH_3CN. A 5 μL amount of dry, oxygen-free acetonitrile (0.09 mmol) was added to a solution of $Cp^*Ir(PMe_3)(S(O)_2CH_3)(OTf)$ (**5**) (22 mg, 0.03 mmol) in CH_2Cl_2-d_2 under an inert atmosphere. Immediate and complete conversion of **5** into $Cp^*Ir(PMe_3)(CH_3CN)(S(O)_2CH_3)^+OTf^-$ (**6**) was observed by NMR spectroscopy. ^1H NMR (400 MHz, CD_2Cl_2): δ 1.82 (d, J_{P-H} = 11.6 Hz, PMe_3), 1.83 (d, J_{P-H} = 2.0 Hz, Cp*), 2.82 (d, J_{P-H} = 1.6 Hz, CH_3), 2.98 (s, CH_3). ^{31}P NMR (400 MHz, CD_2Cl_2): δ −28.95 (s). Anal. Calcd for $C_{17}H_{30}F_3IrNO_5PS_2$: C, 30.36; H, 4.46. Found: C, 30.44; H, 4.49.

Reaction of 2a and 2b with HCl. To a solution of **2a** or **2b** (5 mg, 0.01 mmol) in THF-d_8 was added 0.1 mL of aqueous concentrated HCl (12.5 M, 1.25 mmol). An NMR spectrum taken after a few minutes of reaction shows the clean and complete formation of $(C_5Me_5)Rh(PMe_3)(Cl)_2$ and free sulfinic acid RSO_2H (R = CH_3 or C_6H_5). The sulfinic acids were independently synthesized by reaction of their sodium salts with aqueous concentrated HCl in THF. For CH_3SO_2H, ^1H NMR (400 MHz, THF): δ 2.55 (s, CH_3). For $C_6H_5SO_2H$, ^1H NMR (400 MHz, THF): δ 7.47−7.53 (m, 3 H), 7.63−7.68 (m, 2 H).

Reaction of $Cp^*Rh(PMe_3)(S(O)_2CH_3)(Cl)$ (2b) with HOTf. Increasing amounts of triflic acid (from 1.6 (0.02 mmol) to 6.4 μL (0.07 mmol)) were added to a solution of **2b** (17 mg, 0.04 mmol) in 1 mL of CD_2Cl_2. The changes in the chemical shift of the methyl in the sulfinate group were as follows:

	equiv of HOTf					
	0	0.5	0.7	0.9	1.2	1.8
δ (CH_3) (ppm)	2.82	3.08	3.19	3.27	3.27	3.26

The addition of excess HOTf resulted in the formation of a new compound formulated as $Cp^*Rh(PMe_3)(S(O)(OH)CH_3)(Cl)^+OTf^-$ (**7a**). ^1H NMR (400 MHz, CD_2Cl_2): δ 1.67 (d, J_{P-H} = 12 Hz, PMe_3), 1.74 (d, J_{P-H} = 2.4 Hz, Cp*), 3.27 (s, CH_3), 13.04 (br s, H^+). ^{31}P NMR (400 MHz, CD_2Cl_2): δ 10.77 (br d, J_{Rh-P} = 133 Hz).

Reaction of $Cp^*Rh(PMe_3)(S(O)_2CH_3)(Cl)$ (2b) with HBF_4. A 7.5 μL amount of $HBF_4{\cdot}O(C_2H_5)_2$ (85%, 0.04 mmol) was added to a solution of 10 mg (0.02 mmol) of $Cp^*Rh(PMe_3)(S(O)_2CH_3)(Cl)$ (**2b**) in CD_2Cl_2, giving a new compound $Cp^*Rh(PMe_3)(S(O)(OH)CH_3)(Cl)^+BF_4^-$ (**7b**). ^1H NMR (400 MHz, CD_2Cl_2): δ 1.67 (d, J_{P-H} = 11.6 Hz, PMe_3), 1.74 (d, J_{P-H} = 2.4 Hz, Cp*), 3.23 (s, CH_3), 9.13 (br s, OH). ^{31}P NMR (CD_2Cl_2): δ 10.09 (br s).

Reaction of $Cp^*Rh(PMe_3)(S(O)_2CH_3)(Cl)$ (2b) with Phenyl Sulfinic Acid. A 2 mg (0.014 mmol) amount of $C_6H_5SO_2H$ was added to a solution of 5.4 mg (0.013 mmol) of $Cp^*Rh(PMe_3)(S(O)_2CH_3)(Cl)$ (**2b**) in CH_2Cl_2-d_2. $Cp^*Rh(PMe_3)(S(O)_2C_6H_5)(Cl)$ (**2a**) and CH_3SO_2H were formed. After 2 h at room temperature, the composition of the solution did not change, allowing determination of a value for the equilib-

(9) Jones, W. D.; Feher, F. J. *Inorg. Chem.* **1984**, *23*, 2376−2388.
(10) Buchanan, J. M.; Stryker, J. F.; Bergman, R. G. *J. Am. Chem. Soc.* **1986**, *108*, 1537−1550.

rium constant ($K_{eq} = 0.59$) by integration of the NMR peaks. The addition of more phenyl sulfinic acid (1 mg, 0.007 mmol) led to a change in the composition of the mixture. After 2 h, the composition of the mixture remained constant and a second value for the equilibrium constant was calculated ($K_{eq} = 0.57$).

Reaction of Cp*Rh(PMe$_3$)(CH$_3$)(Cl) (1b) with Triflic Acid. A 3.1 μL amount of triflic acid (0.035 mmol) was added to a solution of 12.6 mg (0.035 mmol) of Cp*Rh(PMe$_3$)(CH$_3$)(Cl) (**1b**) in CH_2Cl_2-d_2 at room temperature. The orange solution turned red immediately. The NMR spectra showed the complete formation of Cp*Rh(PMe$_3$)(Cl)(OTf) (**8**). ^{1}H NMR (400 MHz, CD_2Cl_2): δ 1.60 (d, $J_{P-H} = 11.6$ Hz, PMe$_3$), 1.66 (d, $J_{P-H} = 3.2$ Hz, Cp*). ^{31}P NMR (CD_2Cl_2): δ 8.59 (d, $J_{Rh-P} = 142$ Hz). The addition of excess CH_3SO_2H to **8** in dichloromethane led to the immediate formation of **7a** at room temperature, but 2 days were necessary to form **2b** by reaction of **8** with excess CH_3SO_2Na at room temperature in dichloromethane.

X-ray Structural Determination of (C$_5$Me$_5$)Rh(PMe$_3$)(SO$_2$Ph)Cl, 2a. Golden orange crystals were obtained by layering a CH_2Cl_2 solution of **2a** with hexanes. A single crystal was mounted on a glass fiber with Paratone N. Data were collected at −80 °C on a Siemens SMART CCD area detector system employing a 3 kW sealed-tube X-ray source operating at 1.5 kW. Data (1.3 hemispheres) were collected over 7 h, yielding 11 506 observed data after integration using SAINT (see Table 1). Laue symmetry revealed an orthorhombic crystal system, and cell parameters were determined from 8192 unique reflections.[11] An absorption correction was applied using SADABS. The space group was assigned as $P2_12_12_1$ on the basis of systematic absences using XPREP, and the structure was solved and refined using the SHELX95 package. For a Z value of 4, there is one independent molecule within the asymmetric unit. In the final model, all non-hydrogen atoms were refined anisotropically (on F^2), with hydrogens included in idealized locations. The acentric structure was refined as a racemic twin (0.32/0.68), as the Flack parameter deviated substantially from zero in the initial refinement. Final agreement factors were R1 = 0.0250 and wR2 = 0.0597.[12] Fractional coordinates and thermal parameters are given in the Supporting Information.

X-ray Structural Determination of (C$_5$Me$_5$)Rh(PMe$_3$)(SO$_2$CH$_3$)Cl, 2b. Data collection and structure solution was similar to that described for **2a**. Data (1.3 hemispheres) were collected over 4 h, yielding 10 802 observed data after integration using SAINT (see Table 1). Laue symmetry revealed an orthorhombic crystal system, and cell parameters were determined from 6645 unique reflections.[11] An absorption correction was applied using SADABS. The space group was assigned as $Pna2_1$ on the basis of systematic absences using XPREP, and the structure was solved and refined using the SHELX95 package. For a Z value of 4, there is one independent molecule within the asymmetric unit. In the final model, all non-hydrogen atoms were refined anisotropically (on F^2), with hydrogens included in idealized locations. Final agreement factors were R1 = 0.0396 and wR2 = 0.0663.[12] Fractional coordinates and thermal parameters are given in the Supporting Information.

X-ray Structural Determination of [(C$_5$Me$_5$)Ir(PMe$_3$)(SO$_2$Ph)(CH$_3$CN)]OTf, 6. Data collection and structure solution was similar to that described for **2a**. Data (1.3 hemispheres) were collected over 7 h, yielding 28 131 observed data after integration using SAINT (see Table 1). Laue symmetry revealed a tetragonal crystal system, and cell parameters were determined from 7682 unique reflections.[11] An absorption correction was applied using SADABS. The space group was assigned as $I4_1/a$ on the basis of systematic absences using XPREP, and the structure was solved and refined using the SHELX95 package. For a Z value of 16, there is one independent molecule within the asymmetric unit. In the final model, all non-hydrogen atoms were refined anisotropically (on F^2), with hydrogens included in idealized locations. The triflate counterion was found to be disordered over two locations. In addition, the triflate was found to lie on a 2-fold axis (bisecting the S−C bond), resulting in a rotational disorder that superimposed the CF_3 and SO_3 groups. The CF_3 group showed a 3-fold disorder. In the final model, the positions of the CF_3 and SO_3 groups were constrained to be identical but the atomic positions were permitted to refine along with their thermal parameters. The correct enantiomorph was assigned based upon the value of the Flack parameter (0.02(5)). Final agreement factors were R1 = 0.0816 and wR2 = 0.1869.[12] Fractional coordinates and thermal parameters are given in the Supporting Information.

Acknowledgment is made to the U.S. Department of Energy (Grant No. FG02-86ER13569) for their support of this work. L.L. also thanks Elf Atochem, N. A., for financial support.

Supporting Information Available: Tables of bond distances and angles, atomic positions, and thermal parameters for **2a**, **2b**, and **6** (22 pages). Ordering information is given on any masthead page.

OM971030M

(11) It has been noted that the integration program SAINT produces cell constant errors that are unreasonably small, since systematic error is not included. More reasonable errors might be estimated at 10 times the listed values.

(12) Using the SHELX95 package, $R1 = (\sum||F_o| - |F_c||)/\sum|F_o|$, $wR2 = [\sum[w(F_o^2 - F_c^2)^2]/\sum[w(F_o^2)^2]]^{1/2}$, where $w = 1/[\sigma^2(F_o^2) + (aP)^2 + bP]$ and $P = [f(\text{max of 0 or } F_o^2) + (1 - f)F_c^2]$.